# Consensus Control for Energy Storage Systems with Experimental Validation Using Controller-Hardware-in-the-Loop Testbed

Yin Li, Lingling Fan, Li Bao, Zhixin Miao
*Deparment of Electrical Engineering*
*University of South Florida*
{yin, linglingfan, libao, zmiao}@usf.edu

***Abstract*—Consensus control was proposed by our prior research to maximize the efficiency of microgrid by synchronizing performances of all parallel battery energy storage systems (BESS). The objective of this paper is to validate the performance of consensus control by developing a controller-hardware-in-the-loop testbed which will provide a real-time environment. Besides the validation, this paper will also describes the system topology and the setup process of this testbed in detailed. The testbed emulates a microgrid with three parallel BESS connected to the IEEE-9 bus system. The circuit part is simulated in real-time simulator while the control systems for BESS are implemented in three FPGA-based controllers. Using this testbed, the consensus control was tested under both of grid-connected mode and autonomous mode.**

***Index Terms*—Consensus control, battery energy storage system, controller hardware-in-the-loop, microgrid, distributed control, FPGA-based controller.**

## I. Introduction

As a kind of distributed energy resource (DER), the battery energy storage system (BESS) provides the user with dispatch capability of the renewable energy sources (RES) such as PV and wind [1]. To balance the power and energy in microgrids, BESS stores the energy when the generation is higher than the demand. On the other hand, it supports the system when the demand is higher than the generation. BESS also can improve the reliability of microgrid on the sudden disturbances [1], [2]. However, the disadvantage of BESS is its high costs on the device, maintenance, and depreciation [1]. The depreciation of the battery is inverse proportional to its state of health (SoH) which is influenced by the times of charging and discharging. To minimize the times of charging and discharging, the consensus control was proposed by [3] to synchronize the power and energy of parallel BESS in the microgrid.

Another advantage of the consensus control is the limited data transfer. As a decentralized control, the consensus control only requires each BESS to communicate with its neighbors and the transferred data is only power and energy. Compared with the centralized controls, the consensus control has the lower possibility to be affected by the single point of failure [4], [3], [5]. As a result, the consensus control cannot only reduce the depreciation rate of batteries effectively but also improves the reliability of the microgrid.

978-1-7281-8192-9/21/$31.00 © 2021 IEEE

The consensus control was tested using a pure simulation testbed in [3] but this paper will develop a controller hardware-in-the-loop (CHIL) testbed to evaluate its performance. It is known that the best validation of proposed controls should be implementing them in the real system. However, the high associated costs and risks limit the researchers to test their proposed controls using real systems [6], [7]. As a compromise approach, the hardware-in-the-loop (HIL) testbed is usually developed to provide a practical, safe, and economic environment for the validation. It uses both hardware and software to generate real-time simulation results. When it saves the cost, it can also generate the more practical validations than the pure simulation testbed. HIL simulation has been recognized for the analysis and testing of power system components and it has been widely used to test DERs related studies [6], [7], [8], [9], [10]. When the hardware under test consists only of controllers, this testbed is preferred to as a CHIL [10].

In this paper, a CHIL testbed is developed based on a microgrid with three parallel BESS connected to the standard IEEE 9-bus system. It consists of a real-time simulator (RT-LAB) and multiple FPGA-based controllers. RT-LAB is used to emulate the circuit part including the IEEE 9-bus system and three parallel BESS while the FPGA-based controllers are used to generate the control signals for BESS. The control system of each BESS includes a conventional $PQ$ control and the consensus loop as the top layer. To achieve the consensus, the FPGA-based controller needs to communicate with both the real-time simulator and its neighboring controllers via the physical connections. The case study does not validate the performance of the consensus control under the grid-connected mode but also validates it under the autonomous mode and the transient between two modes.

The rest of the paper is organized as the follows. In Section II, the design of the consensus control for the three parallel BESS will be introduced. In Section III, the configuration of CHIL testbed will be presented in details. In Section IV, the experimental results are plotted to validate the performance of the consensus control under both connection mode.

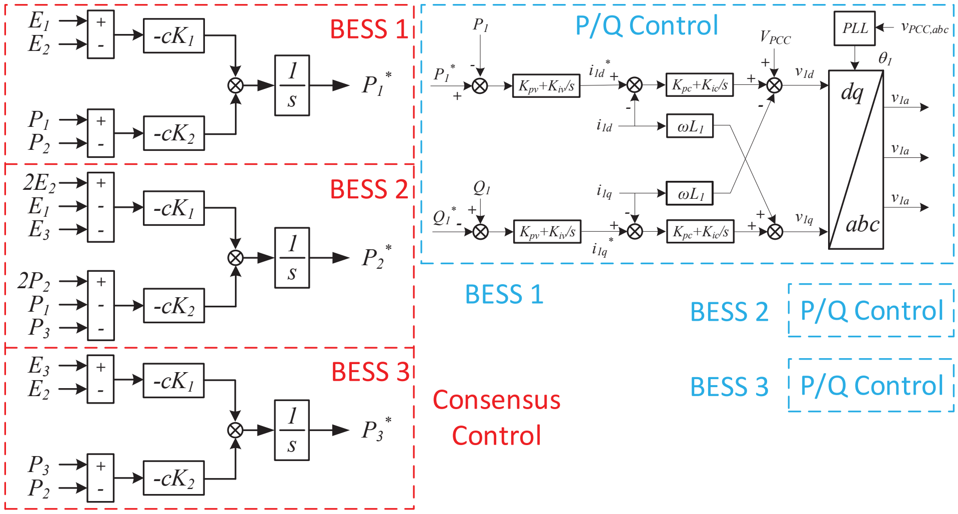


Fig. 1: Control strategies for three BESS.

## II. Consensus control design

The communication network is important to design the consensus control because it requires the data transferred. Fig. 2 shows the communication graph of a three-BESS microgrid studied in this paper. It can be expressed by Laplacian matrix *L*. *D* matrix represents the degree of each node while *A* matrix represents the communication link between each two nodes. As its advantage, consensus control only requires each BESS to communicate with its neighbors.

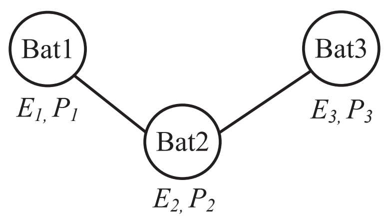


Fig. 2: Three-energy-storage system.

$$L = \begin{bmatrix} 1 & -1 & 0 \\ -1 & 2 & -1 \\ 0 & -1 & 1 \end{bmatrix} = \underbrace{\begin{bmatrix} 1 & 0 & 0 \\ 0 & 2 & 0 \\ 0 & 0 & 1 \end{bmatrix}}_{D} - \underbrace{\begin{bmatrix} 0 & 1 & 0 \\ 1 & 0 & 1 \\ 0 & 1 & 0 \end{bmatrix}}_{A} \quad (1)$$

Due to the relation between energy and power, the dynamics of each BESS can be written by (2).

$$\underbrace{\begin{bmatrix} \dot{E}_1 \\ \dot{P}_1 \end{bmatrix}}_{\dot{x}_i} = \underbrace{\begin{bmatrix} 0 & -1/3600 \\ 0 & 0 \end{bmatrix}}_{A} \underbrace{\begin{bmatrix} E_1 \\ P_1 \end{bmatrix}}_{x_i} + \underbrace{\begin{bmatrix} 0 \\ 1 \end{bmatrix}}_{B} u_i \quad (2)$$

where $E_i$ and $P_i$ indicate the energy and power of $i$th BESS. The energy and power are the states while the differential of power is the input $u_i$. Note that the energy can also be represented by the state of charge (SoC).

To achieve the consensus on energy and power of all BESS, the control input is designed as the following equation [11].

$$u_i = cK \sum_{j=1}^{N} a_{ij}(x_j - x_i) \quad (3)$$

where $c$ is a positive scalar coupling gain, $K$ is the feedback control matrix, and $a_{ij}$ is the element of $A$ matrix. $N$ is the total number of BESS and it is 3 in this paper. With this design, the sum of inputs is always zero. Because the input is the differential power of each BESS, the design forces the sum of real power of all BESS to be a constant.

Linear quadratic regulator (LQR) with the infinite-horizon is used to find the feedback gain matrix *K* which minimizes the sum of the inputs.

$$K = R^{-1} B^T P_{uni} \quad (4)$$

$$u = -cKx \quad (5)$$

where $P_{uni}$ is the unique positive definite solution of the control algebraic Riccati equation (ARE). The following equation is the continue-time ARE.

$$A^T P_{uni} + P_1 A + Q - P_{uni} B R^{-1} B^T P_1 = 0 \quad (6)$$

where $Q$ and $R$ are two weight matrices. After $Q$ and $R$ are given, this equation can be solved to find $P_{uni}$ by MATLAB code *care*; then, *K* can be calculated. In other words, the design of $Q$ and $R$ will affect the performance of consensus control. According to [3], a larger $Q$ results in faster dynamic response in $x_i$ while a larger $R$ penalizes the input and results in less effort in control or small values in $u_i$.

The scalar coupling gain $c$ should be design to make the system stable. The following equation shows the maximum value which can be selected for $c$.

$$c \leq \max\left(\frac{1}{2\min Re(\lambda_i)}, 1\right) \; i = 2, ..., n \quad (7)$$

where $\lambda_i$ is the eigenvalue of $L$ matrix.

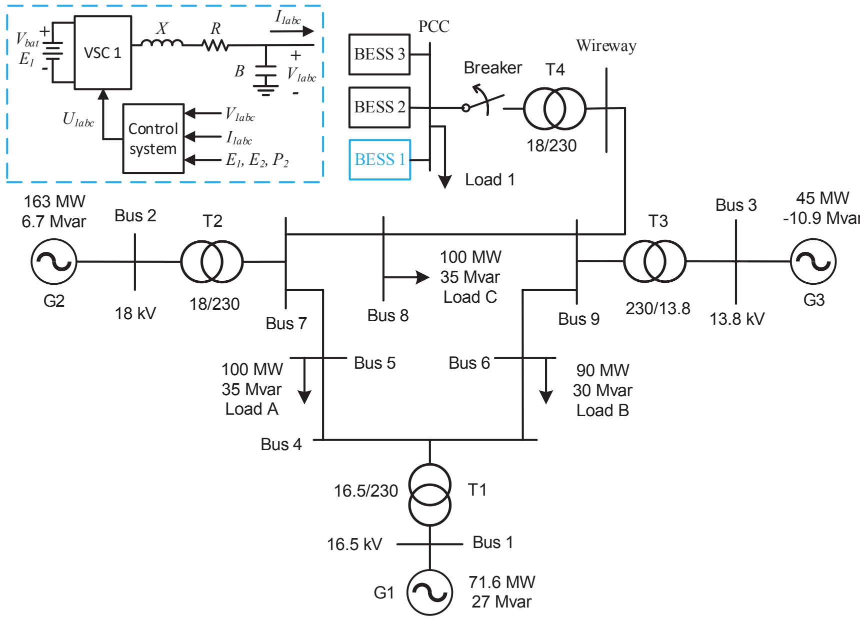


Fig. 3: The microgrid including three energy storage systems is integrated to IEEE-9 Bus system.

After designing the part of the consensus control, we need to implement it upon the conventional vector control. The input $u_i$ needs to be integrated as the power reference which is sent to the outer loop of vector control. Hence, the real power of BESS should be controllable. Fig. 1 shows the control strategies for three BESS under the grid-connected mode. The consensus part is boxed by the red line while the vector control is boxed by the blue line. Each BESS employs a conventional vector control to control its output power, $P$ and $Q$. The reference of the real power is from the consensus part. The parameters selected for the control system are listed in Table I.

## III. CHIL TESTBED

To evaluate the performance of the consensus control, the controller-hardware-in-the-loop testbed is built to emulate a three-BESS microgrid integrated to the large-scale system. It consists of a real-time simulator (RT-LAB) and three FGPA-based controllers. This section will describe the configuration of this testbed.

### A. Topology of circuit

The topology of circuit is shown in Fig. 3. A microgrid with three battery energy storage systems is integrated to grid. The grid is represented by IEEE 9-bus system including three synchronous generators and three loads. The parameters of IEEE-9 bus system are from the standard 9 bus system data [12] and are listed in Table II. The microgrid is integrated at Bus 9 through a transformer $T4$ which is same as $T2$. Three BESS and one load are connected at the point of the common coupling (PCC) bus in parallel. The details of BESS 1 are circiled by the blue dashed line in Fig. 3. A $LC$ filter is utilized between the inverter and the PCC bus. The inverter used in BESS is the average model which uses the controllable three-phase voltage source instead of the dynamics of IGBTs. A breaker is used between the transformer and the PCC bus to switch the the connection mode of the microgrid. The parameters of the microgrid are presented in Table I.

### B. Configuration of testbed

The configuration of CHIL testbed is shown in Fig. 4. The circuit shown in Fig. 3 is simulated in RT-LAB including IEEE 9-bus system and three-BESS microgrid. In addition, the turbine governors for synchronous generators are simulated in RT-LAB as well. The series number of RT-LAB is OP5600. The control loops for three BESS shown in Fig. 1 are designed on three FPGA-based controllers respectively.

The FPGA-based controller used in this testbed is from National Instrument (NI). It actually includes three pieces of boards. The lower piece is named as mini-scale SKiiP3 Replica Back-to-Back Converter board. We used the analog and digital ports on this board to transfer signals. The upper piece is the single-board real-time input/output (sbRIO 9606) including both of FPGA-based digital controller and NI general purpose inverter controller (GPIC). They are used to control all inputs and outputs on the lower piece. The middle piece is the bridge to connect another two boards. The FPGA-based controller can be programmed by NI application LabVIEW.

The communications between RT-LAB and sbRIOs are based on the analog input/output. The communication paths and transferred signals are labeled in Fig. 4. RT-LAB sends the energy or SoC $E_i$ and three-phase instantaneous voltages $V_{iabc}$ and currents $I_{iabc}$ to sbRIOs for the vector control. The power measurements $P_i$ are calculated in the sbRIOs based on $V_{iabc}$ and $I_{iabc}$. To achieve the consensus, sbRIOs also need to communicate with their neighboring controllers to transfer $P_i$ and $E_i$. After the process of consensus controls, sbRIOs send the instantaneous control voltages $U_{iabc}$ back to RT-LAB in three phases to control inverters.

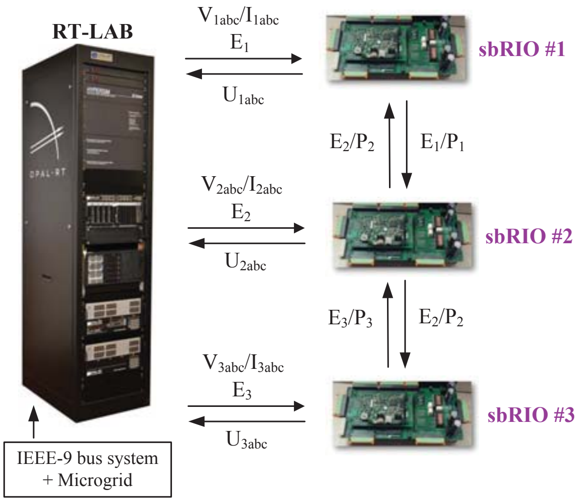


Fig. 4: The overview of CHIL testbed.

Fig. 5a shows the overview of our CHIL testbed. Besides real-time simulator and FPGA-based controllers, two host PCs are used to control these two types of devices respectively. During the simulation, the graphic user interfaces (GUIs) of both RT-LAB and LabVIEW can be used to monitor the measurements and send comments to the testbed such as triggering the breaker. Fig. 5b zooms in the construction of three sbRIOs which are overlaid one by one. The communication between devices are based on the 37−Pin D-Sub cables.

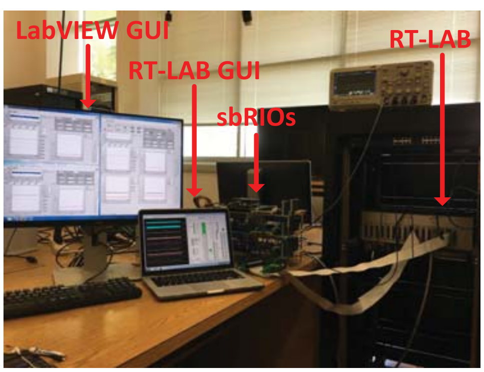


(a)

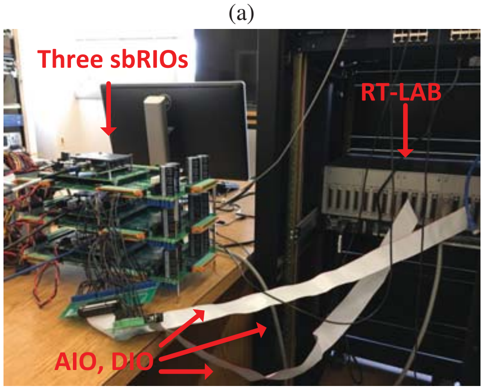


(b)

Fig. 5: (5a) The photo of CHIL testbed built in our lab. (5b) zoom-in photo to show the detailed connections of RT-LAB and sbRIOs.

## IV. Experimental Results

In this section, the consensus control was tested under two modes, the grid-connected mode and autonomous mode. When the microgrid was connected to IEEE 9-bus system, three BESS belonged to grid-following inverter-based resources (IBRs) under $P/Q$ control. The control loops were the same as Fig. 1. After the breaker became open, the microgrid was disconnected the grid. At this moment, we selected BESS 1 to forming the PCC voltage and the system frequency so it became the grid-forming inverter by switching its control mode from $P/Q$ control to $V/f$ control. It means that the power of BESS 1 could not be controlled under autonomous mode. Hence, the consensus control only coordinated BESS 2 and BESS 3 under the autonomous mode. Because BESS 2 did not need to communicate with BESS 1, the consensus loop of BESS 2 needed to be changed. As a result, the control loops under autonomous mode are shown in Fig. 6.

Under both modes, the energy signal and power signal of each BESS were plotted to present the dynamics of microgrid. For IEEE 9-bus system, the dynamics at Bus 1, 2, and 3 were plotted including frequencies, voltage magnitudes, real power, and reactive power. The simulation was not stopped until the energy and power signals converged.

### A. Grid-connected mode

Under the grid-connected mode, three BESS totally generated 90 MW real power. In detailed, BESS 1 generated 50 MW real power while BESS 2 and BESS 3 generated 20 MW real power each. Because of a 50 MW resistive load integrated at PCC bus, the microgrid totally transferred 40 MW power to the IEEE 9-bus system under the grid-connected mode. To keep the standard power flow of IEEE 9-bus system, the real power generated by Generator 3 was reduced by 40 MW. At the initial condition, the SoC of three BESS are 0.9 pu, 0.8 pu, and 0.85 pu

Fig. 7a shows the dynamics of BESS. Before 60 sec, inverters in BESS were still controlled by the control loops in RT-LAB. At 60 sec. sbRIOs were activated to receive and send signals with RT-LAB. Due to the communication between sbRIOs and RT-LAB based on the physical cables and ports, the obvious noise appeared in the dynamic response from 60 sec. At 130 sec, the consensus control was activated for all BESS so their power references were controlled by the consensus loops rather than constants. Around 1100 sec, the power signals of three BESS were converged at 30 MW and the energy signals were converged as well.

Based on Fig. 7b, we can observe the large disturbance which was caused by sbRIOs joined in. However, the effect of consensus control on the IEEE 9-bus system was slight because the power flow in IEEE 9-bus system was not changed. The total power generated by three BESS was still 90 MW and the total power transferred to the IEEE 9-bus system was still 40 MW.

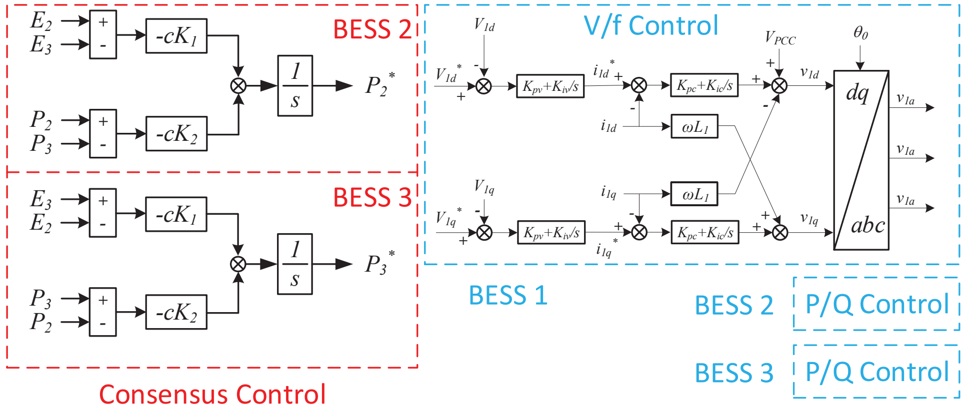


Fig. 6: Control strategies for three BESS under the autonomous mode.

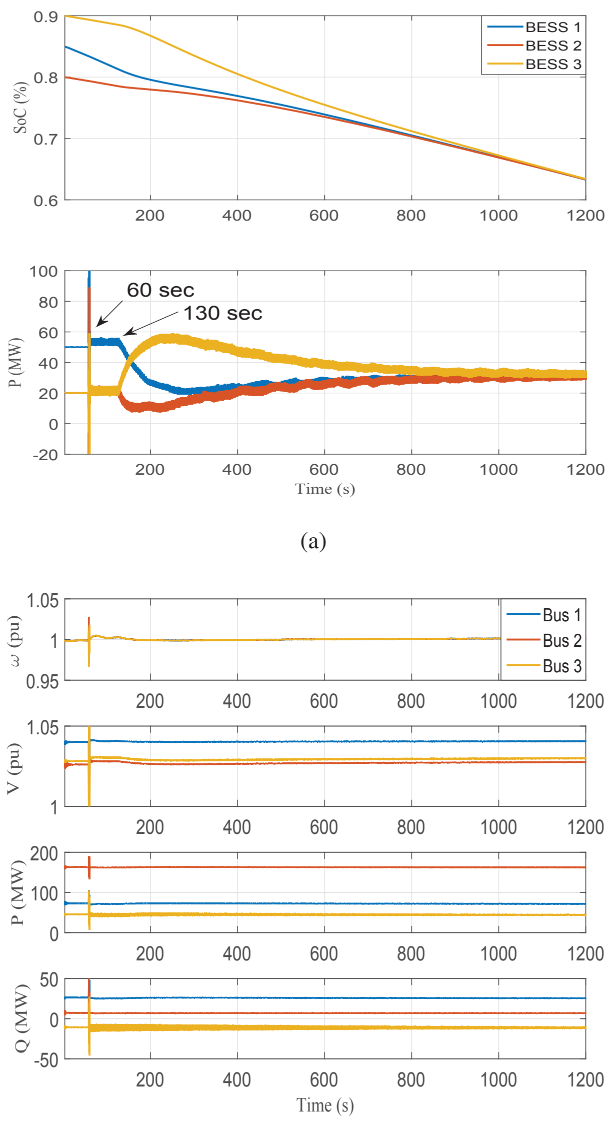


(a)

(b)

Fig. 7: Real-time simulation results under grid-connected mode. 7a Dynamics of BESS. 7b Dynamics of IEEE 9-bus system.

### B. *Autonomous mode*

In thie case, the microgrid was disconnected from the IEEE 9-bus system at 225 sec. Fig. 8a shows the transient dynamics of the microgrid which was switched from the grid-connected mode to the autonomous mode.

At 55 sec, sbRIOs started to control inverters of BESS. At 108 sec, the consensus control was activated for three BESS. At this moment, the microgrid was still connected to the IEEE 9-bus system so all three BESS started to approach the consensus on the power and energy. At 225 sec, the microgrid was disconnected from the IEEE 9-bus system. BESS 1 was switched to $V/f$ control mode while BESS 2 and BESS 3 were still under $PQ$ control mode. At this moment, the consensus control was switched to the strategies in Fig. 6 and the initial power references were reset. Based on the initial power references, BESS 2 and BESS 3 still needed to generate 20 MW respectively while BESS 1 only needed to generate 10 MW because of the 50 MW load. Therefore, right after the microgrid disconnected, the power measurements of BESS 2 and BESS 3 were reduced to 20 MW while the power of BESS 1 was reduced to 10 MW. Then, the power and energy of BESS 2 and BEES 3 were converging because the consensus control only coordinated both VSC 2 and VSC 3 after 220 sec. Based on Fig. 8a, we found that the energy and power of BESS 2 and BESS 3 were converged after 1100 sec.

In this case, the change of connection mode of microgrid also affected the IEEE 9-bus system. It caused that IEEE 9 bus system lost 40 MW real power from the microgrid. As shown in Fig. 8b, although three synchronous generators generated more power, the power generation was still lower than power demand. Hence, it resulted in 3% drop of the frequency of the IEEE 9 bus system.

## V. Conclusion

Consensus control was proposed by our previous work to achieve the consensus on energy and power of multiple BESS in the microgrid. In this paper, the consensus control was implemented in a controller hardware-in-the-loop testbed for the evaluation. It provides the detailed procedures on constructing the testbed including the controls, parameters,

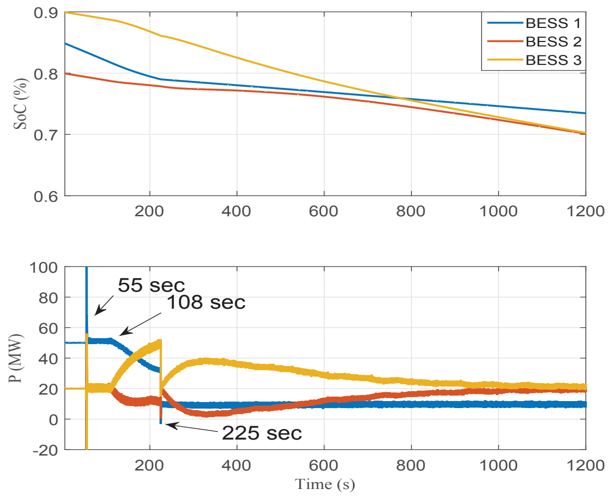


(a)

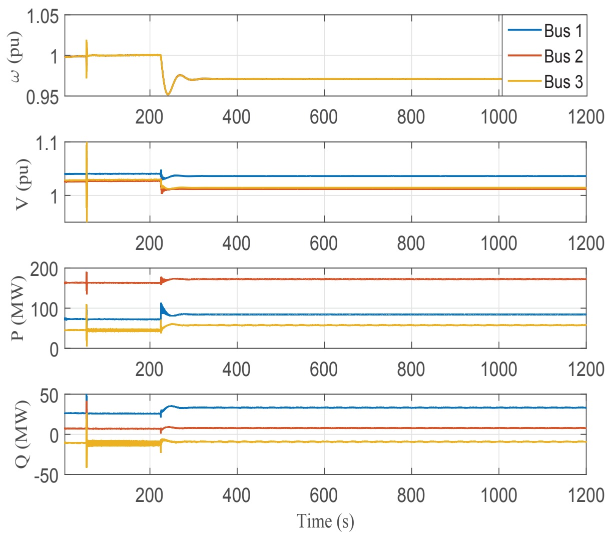


(b)

Fig. 8: Real-time simulation results under islanded mode. 8a Dynamics of BESS. 8b Dynamics of IEEE 9-bus system.

and connections. With this testbed, the consensus control was tested under the grid-connected mode, autonomous mode, and the transient of connection mode change. The real-time simulation results validated the good performance of consensus control in microgrids. In the future, the capability of the microgrid with the consensus control on the disturbance in the large-scale power system can be evaluated. Furthermore, other coordinate controls can be implemented in this CHIL testbed for the evaluations.

## Appendix

TABLE I: Parameters of the microgrid

| Names | values |
|---|---|
| $S_b$ | 100 MVA |
| $V_b$ at grid | 230 kV |
| $V_b$ in microgrid | 18 kV |
| $X, R, B$ | 0.1, 0.02, 0.05 |
| $X_T$ | 0.0675 |
| $K_{pc}$, $K_{ic}$ | 0.3, 5 |
| $K_{pv}$, $K_{iv}$ | 0.25, 25 |
| $K_{ipll}$, $K_{ipll}$ | 60, 1400 |
| Q | diag([800,10]) |
| R | 2 |
| $K_1$ | -20 |
| $K_2$ | 0.715 |
| c | 0.01 |

TABLE II: Parameters of IEEE 9-bus

| Generator # | 1 | 2 | 3 |
|---|---|---|---|
| Rated MVA | 247.5 | 192.0 | 128.0 |
| Rated kV | 16.5 | 18.0 | 13.8 |
| $X_T$(pu) | 0.0576 | 0.0675 | 0.0586 |
| Lines | R(pu) | X(pu) | B/2(pu) |
| Bus4-Bus5 | 0.010 | 0.085 | 0.088 |
| Bus4-Bus6 | 0.017 | 0.092 | 0.079 |
| Bus5-Bus7 | 0.032 | 0.161 | 0.153 |
| Bus6-Bus9 | 0.039 | 0.170 | 0.179 |
| Bus7-Bus8 | 0.0085 | 0.072 | 0.0745 |
| Bus8-Bus9 | 0.0119 | 0.1008 | 0.1045 |

## References


[1] A. M. Bouzid, J. M. Guerrero, A. Cheriti, M. Bouhamida, P. Sicard, and M. Benghanem, "A survey on control of electric power distributed generation systems for microgrid applications," *Renewable and Sustainable Energy Reviews*, vol. 44, pp. 751 – 766, 2015. [Online]. Available: http://www.sciencedirect.com/science/article/pii/S136403211500026X

[2] C. A. Hill, M. C. Such, D. Chen, J. Gonzalez, and W. M. Grady, "Battery energy storage for enabling integration of distributed solar power generation," *IEEE Transactions on Smart Grid*, vol. 3, no. 2, pp. 850–857, June 2012.

[3] J. Khazaei and Z. Miao, "Consensus control for energy storage systems," *IEEE Transactions on Smart Grid*, vol. 9, no. 4, pp. 3009–3017, July 2018.

[4] N. Prabaharan, A. R. A. Jerin, E. Najafi, and K. Palanisamy, "6 - an overview of control techniques and technical challenge for inverters in micro grid," in *Hybrid-Renewable Energy Systems in Microgrids*, ser. Woodhead Publishing Series in Energy, A. H. Fathima, N. Prabaharan, K. Palanisamy, A. Kalam, S. Mekhilef, and J. J. Justo, Eds. Woodhead Publishing, 2018, pp. 97 – 107.

[5] A. Tuckey, S. Zabihi, and S. Round, "Decentralized control of a microgrid," in *2017 19th European Conference on Power Electronics and Applications (EPE'17 ECCE Europe)*, Sep. 2017, pp. P.1–P.10.

[6] E. Limpaecher, R. Ulerio, E. Corbett, S. Manson, B. Nayak, and W. Allen, "Lessons learned from hardware-in-the-loop testing of microgrid control systems," *CIGRE 2017 Grid of the Future Symp*, Oct. 2017.

[7] O. Azofeifa, S. Nigam, O. Ajala, C. Sain, S. Utomi, A. D. Domínguez-García, and P. W. Sauer, "Controller hardware-in-the-loop testbed for distributed coordination and control architectures," in *2019 North American Power Symposium (NAPS)*, Oct 2019, pp. 1–6.

[8] P. Kotsampopoulos, D. Lagos, N. Hatziargyriou, M. O. Faruque, G. Lauss, O. Nzimako, P. Forsyth, M. Steurer, F. Ponci, A. Monti, V. Dinavahi, and K. Strunz, "A benchmark system for hardware-in-the-loop testing of distributed energy resources," *IEEE Power and Energy Technology Systems Journal*, vol. 5, no. 3, pp. 94–103, Sep. 2018.

[9] K. Prabakar, M. Shirazi, A. Singh, and S. Chakraborty, "Advanced photovoltaic inverter control development and validation in a controller-hardware-in-the-loop test bed," in *2017 IEEE Energy Conversion Congress and Exposition (ECCE)*, Oct 2017, pp. 1673–1679.

[10] M. Steurer, F. Bogdan, W. Ren, M. Sloderbeck, and S. Woodruff, "Controller and power hardware-in-loop methods for accelerating renewable energy integration," in *2007 IEEE Power Engineering Society General Meeting*, June 2007, pp. 1–4.

[11] A. Bidram, A. Davoudi, F. L. Lewis, and J. M. Guerrero, "Distributed cooperative secondary control of microgrids using feedback linearization," *IEEE Transactions on Power Systems*, vol. 28, no. 3, pp. 3462–3470, Aug 2013.

[12] A. F. P.M. Anderson, *Power System Control and Stability*. Iowa State University Press.